Supporting information

Agglomeration of viruses by cationic lignin particles for facilitated water purification

Guillaume N. Rivière,[1] Antti Korpi, [1] Mika Henrikki Sipponen, [1,2] Tao Zou, [1] Mauri A. Kostiainen, [1] and Monika Österberg[1]**

[1]Department of Bioproducts and Biosystems, Aalto University, P.O. Box 16300, FI-00076 Aalto, Espoo, Finland

[2]Current address: Department of Materials and Environmental Chemistry, Stockholm University, Svante Arrhenius väg 16C, 106 91 Stockholm, Sweden

*Corresponding authors:

monika.osterberg@aalto.fi

mika.sipponen@mmk.su.se

Total Pages: 12

Total number of Figures: 6

Total number of Tables: 5

Table S1 shows quantitative ^{31}P NMR results of softwood kraft lignin and the corresponding water-soluble fraction of (quaternary ammonium derivatized) cationic lignin. This data shows that glycidyltrimethyl ammonium chloride (GTMAC) used in the cationization reaction reacted preferentially with aliphatic hydroxyl groups and phenolic hydroxyl groups of softwood kraft lignin.

Table S1. ^{31}P NMR analysis of softwood kraft lignin and the corresponding cationized lignin. Amounts are in mmol g^{-1}. Data was reproduced from a previous study.[41]

Type of lignin	**Aliphatic**	**COOH**	**H** [a]	**G** [b]	**Total phenolic**
Softwood kraft lignin	1.89±0.05	0.57±0.07	0.31±0.02	3.74±0.02	4.05±0.04
Cationic lignin	2.64±0.04	0.61±0.23	0.10±0.02	1.32±0.05	1.42±0.03

Pooled percentage errors relative to the means (N=2) were 1% (pine kraft lignin) and 4% (cationic lignin).

Table S2 presents the particle properties for the second batch of anionic and cationic lignin particles. Although the size of the particles is different compared to the batch utilized for the DLS, AFM and TEM, it was more important to the virus agglomeration studies that the zeta potential values were very similar. The ratio of cationic lignin to CLPs was higher (300 mg g^{-1}) due to the smaller size of the particles. The first batch was used for DLS, AFM and titration experiments while the second batch was used for the virus removal in different salt conditions and filtration experiments.

Table S2. Characterization of the different batches of CLPs and c-CLPs utilized for the study. Values obtained in water.

Type of lignin dispersion	Batch number	Hydrodynamic diameter (nm)	PDI	Zeta potential (mV)
CLPs	1	108.6 ± 1.7	0.065 ± 0.020	-35.9 ± 1.6
	2	70.8 ± 1.1	0.112 ± 0.021	-37.2 ± 1.1
c-CLPs	1	122.4 ± 0.5	0.056 ± 0.005	+24.1 ± 1.4
	2	103.2 ± 0.6	0.167 ± 0.015	+19.2 ± 1.1

Table S3 shows the absorbance of the supernatant under the conditions of the titration experiments of c-CLPs on CCMVs. Absorbance of 0.5 at 260 nm was used as a starting point for solution containing only viruses (before and after centrifugation). Thus, it was important to ensure that the influence of c-CLP was negligible. Before washing, the supernatant containing only c-CLPs presented an absorbance of 0.343, meaning that the effect on virus removal could not be clearly seen. However, after washing, the absorbance measured was only of 0.018. This work was done directly with the highest lignin concentration tested to ensure that the washing was efficient during all experiments. In addition, the Zeta potential of the c-CLP dispersions before and after the washing is compared. The results shows a slight reduction of the charge after the washing in 10 mM NaOAc buffer, however the particles were still cationic enough for our study. This reduction was mainly due to the removal of the water-soluble cationic lignin in excess which was not adsorbed on the CLP surface.

Table S3. Absorbance of supernatant from c-CLP dispersion (0.34 mg/ml) at 260 nm before and after washing with aqueous buffer solution and Zeta potential of the c-CLP dispersion. Error ranges are standard deviations.

	A (260 nm)	**Zeta potential (mV)**
Before washing	0.343 ± 0.139	19.1 ± 1.0 [a]
After washing	0.018 ± 0.006	14.7 ± 1.7 [b]

Values collected at [a] pH 4.2 and [b] pH 5

Figure S1a shows the size distribution by intensities of c-CLPs, CCMVs and c-CLP:CCMV complexes. The autocorrelation function presented in Figure S2b shows the raw data collected by the light scattering equipment. The faster the signal decay the smaller are the particles. Additionally, the smooth curves obtained prove that the samples are monodispersed.

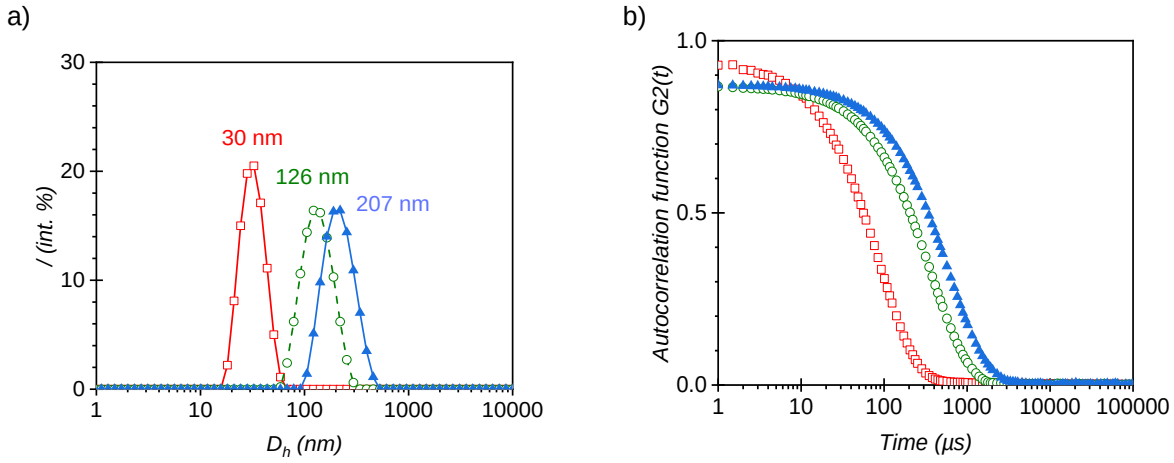

Figure S1. a) Size distribution by intensities and **b)** autocorrelation function of CCMVs (red line and squares), c-CLPs (green line and circles) and c-CLP:CCMV complex (blue line and triangles) in deionized water.

Figure S2 presents the analysis of CCMV-c-CLP interactions based on the Langmuir adsorption isotherm. Figure S3a, shows that no plateau was reached even at higher concentration of CCMVs. In Figure S3b, the adsorption isotherm does not show a good fit to the Langmuir monolayer adsorption equation, suggesting that the interactions between c-CLPS and CCMVs was not purely based on monolayer adsorption of CCMV on c-CLPs.

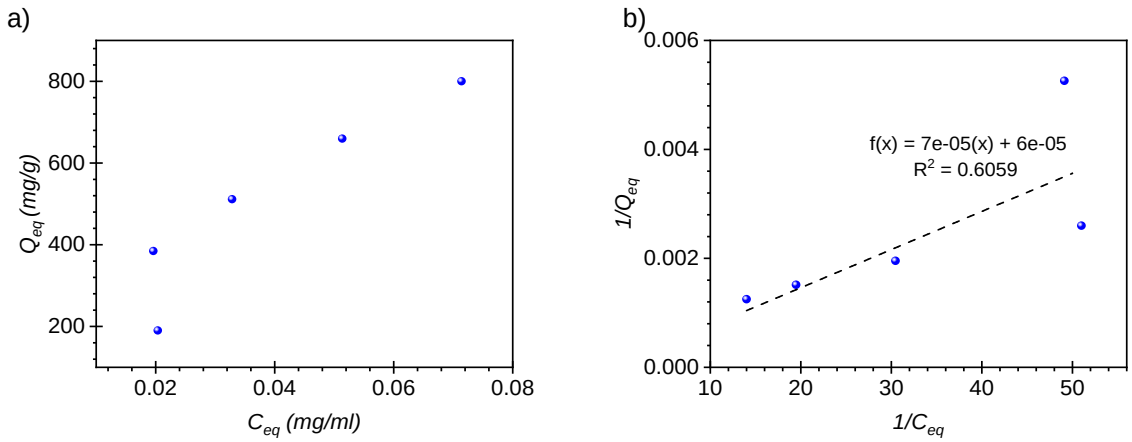

Figure S2. a) Adsorption isotherm of CCMVs on c-CLPs. **b)** Correlation with Langmuir equation

Table S4 shows the overall results from a Two-way ANOVA study on Origin software. This study was used to determine if the results obtained for the removal of viruses by centrifugation (at ratio 2:1 of c-CLPs and CCMVs) were significantly different and if relevant, to determine what factor influence the results. The factors defined for comparison were the charge of the lignin particles and the presence of salts (these factors are respectively called "Lignin" and "Salt" in the table S4). Thus, the conclusions were: At the 0.05 level, the population means of Salt are not significantly different. At the 0.05 level, the population means of Lignin are significantly different. At the 0.05 level, the population means of Lignin are significantly different. At the 0.05 level, the population means of Lignin are significantly different. At the 0.05 level, the interaction between Salt and Lignin is not significantly different. These conclusions mean that the most influential factor was the charge of the lignin particles and not the presence of salt in the mixture.

Table S4. Overall ANOVA results

	DF	Sum of Squares	Mean Square	F Value	P Value
Salt	3	0.11193	0.03731	1.86894	0.1658
Lignin	1	0.15917	0.15917	7.97303	0.01017
Interaction	3	0.09963	0.03321	1.66346	0.20527
Model	7	0.32227	0.04604	2.3061	0.0654
Error	21	0.41923	0.01996	--	--
Corrected Total	28	0.7415	--	--	--

Figure S3 shows the full UV-vis spectra of aqueous dispersions of c-CLPs, CCMVs and c-CLP:CCMV complexes at ratio of 4:1. No significant differences in the spectra recorded from CCMVs before and after filtration through 0.45 µm membrane were observed. However, a decrease of absorbance was observed for c-CLPs alone and the mixture. This suggests that the c-CLPs aggregated in water and assisted the removal of viruses.

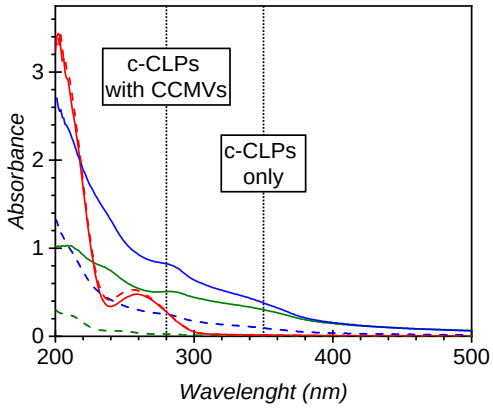

Figure S3. UV-vis spectra of c-CLPs (green), CCMVs (red) and c-CLP:CCMV complex (blue) before filtration (full lines) and after filtration (dashed lines).

Table S5 shows width and height of particles (CCMVs and c-CLPs, individually and as mixtures) using the section tool from Nanoscope Analysis software. Several particles were measured and the average is presented in the table with their error ranges. Similar particle sizes were observed in individual samples and in complexed samples, thus viruses and lignin particles can be clearly identified. Due to the drying, the particles were slightly larger and flatter than observed from DLS measurements (results presented in the main manuscript).

Table S5. Determination of height and width from AFM by section of particles. Error ranges are standard deviations.

	Isolated CCMVs	**Isolated c-CLPs**	**Complexed CCMVs**	**Complexed c-CLPs**
Width	44 ± 3	169 ± 8	44 ± 2	142 ± 12
Height	6 ± 2	62 ± 14	10 ± 4	51 ± 24

Figure S4 shows AFM images of the CLP:CCMV complexes with similar aggregation behavior than detected with the c-CLP:CCMV complexes. It seems that CCMVs can be observed on the surface of the CLPs (Figure S5c).

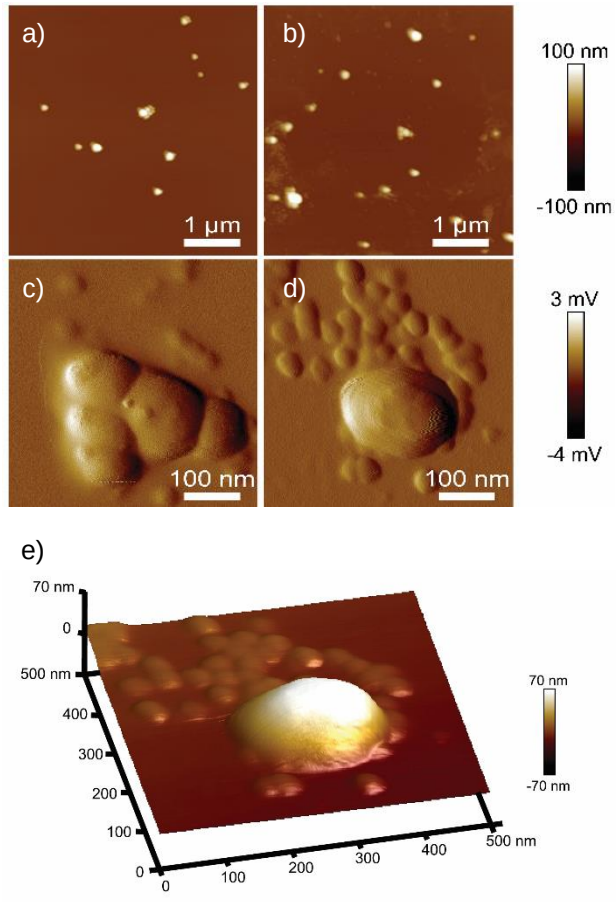

Figure S4. a) AFM height image of CLP dispersion and **b)** CLP:CCMV complexes. **c)** and **d)** Amplitude images of CLP:CCMV complexes. **e)** 3D height image from image **d)**.

Figure S5 and Figure S6 are additional TEM images collected from the samples containing anionic CLPs and viruses. Without the negative staining the viruses were not clearly identified. But it seems that distortions of CLPs are visible, as observed in the main manuscript. Nonetheless, it cannot be ruled out that these observations are due to drying effect or buffer effect.

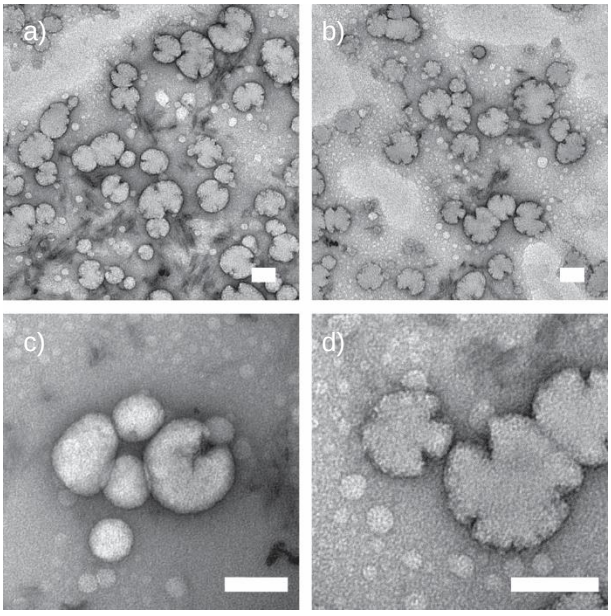

Figure S5. TEM images with negative staining of CLPs with CCMVs. All scale bars: 100 nm

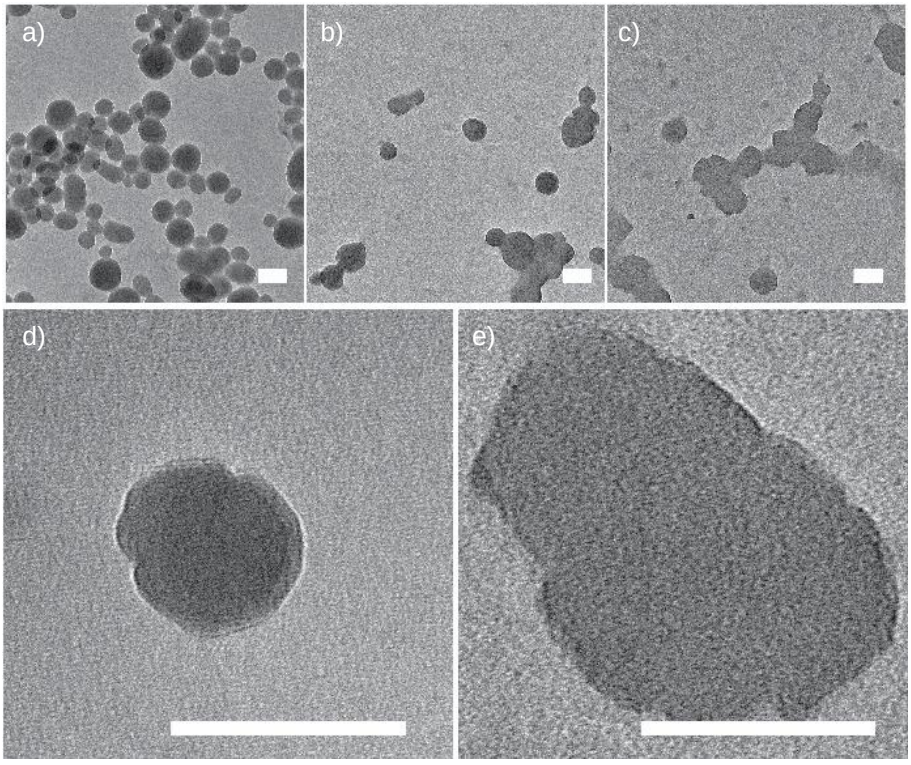

Figure S6. TEM images without staining of **a)** CLPs and from **b)** to **e)** CLP:CCMV complexes.

All scale bars: 100 nm.